Myelin-specific CD8+ T cells exacerbate brain inflammation in CNS autoimmunity

Catriona A. Wagner,[1] Pamela J. Roqué,[1] Trevor R. Mileur,[1] Denny Liggitt,[2] and Joan M. Goverman[1]

[1]Department of Immunology and [2]Department of Comparative Medicine, University of Washington, Seattle, Washington, USA.

Multiple sclerosis (MS) is an inflammatory, demyelinating disease of the CNS. Although CD4+ T cells are implicated in MS pathogenesis and have been the main focus of MS research using the animal model experimental autoimmune encephalomyelitis (EAE), substantial evidence from patients with MS points to a role for CD8+ T cells in disease pathogenesis. We previously showed that an MHC class I–restricted epitope of myelin basic protein (MBP) is presented in the CNS during CD4+ T cell–initiated EAE. Here, we investigated whether naive MBP-specific CD8+ T cells recruited to the CNS during CD4+ T cell–initiated EAE engaged in determinant spreading and influenced disease. We found that the MBP-specific CD8+ T cells exacerbated brain but not spinal cord inflammation. We show that a higher frequency of monocytes and monocyte-derived cells presented the MHC class I–restricted MBP ligand in the brain compared with the spinal cord. Infiltration of MBP-specific CD8+ T cells enhanced ROS production in the brain only in these cell types and only when the MBP-specific CD8+ T cells expressed Fas ligand (FasL). These results suggest that myelin-specific CD8+ T cells may contribute to disease pathogenesis via a FasL-dependent mechanism that preferentially promotes lesion formation in the brain.

Introduction

Multiple sclerosis (MS) is an autoimmune disease of the CNS that affects approximately 2.3 million people worldwide (1). MS is characterized by inflammatory multifocal lesions, plaques of demyelination, and oligodendrocyte loss (2). CD4+ T cells are implicated in the pathogenesis of MS by the strong association of disease susceptibility with MHC class II alleles (3). Furthermore, experimental autoimmune encephalomyelitis (EAE), a widely used animal model of MS, is induced by activation of myelin-specific CD4+ T cells (4). Many insights into the potential mechanisms underlying the pathogenesis of MS have emerged from studies using EAE. Nevertheless, some features of MS are not well recapitulated in EAE. In contrast to MS, in which lesions are commonly seen in the brain, the spinal cord is preferentially targeted for inflammation and the brain is relatively spared of parenchymal lesions in most murine EAE models (5). Differences in the effector functions of CD4+ T cells that mediate EAE versus MS may provide one explanation for this discrepancy. Work from our laboratory and others has shown that the relative amounts of the cytokines IL-17, IFN-γ, and GM-CSF produced by CD4+ T cells influence lesion distribution between the brain and spinal cord in EAE (6). IL-17, IFN-γ, and GM-CSF all promote spinal cord inflammation resulting in "classic" EAE symptoms of ascending flaccid paralysis. IL-17 and GM-CSF also promote inflammation in the brain, resulting in "atypical" EAE symptoms of ataxia, leaning, and axial rotation (7–9). In contrast, IFN-γ inhibits brain inflammation in EAE (10).

Thus, one reason that the spinal cord may be preferentially targeted in EAE is that IFN-γ–producing CD4+ T cells may predominate in the pathogenesis of the animal model but not in patients with MS, although the effector functions of pathogenic CD4+ T cells in MS have not yet been defined. Other factors may also contribute to promoting brain versus spinal cord inflammation in MS that have not yet been identified.

Another limitation of EAE is that the methods used to initiate disease focus exclusively on the activity of CD4+ T cells. EAE is induced either by immunization with myelin antigen, which preferentially results in antigen presentation in the MHC class II pathway, or by adoptive transfer of myelin-specific CD4+ T cells (11, 12). However, there is substantial evidence implicating CD8+ T cells in the pathogenesis of MS. CD8+ T cells are the predominant lymphocyte seen in CNS lesions of MS patients (13, 14). Clonal expansion is more commonly observed among CD8+ compared with CD4+ T cells, suggesting that antigen-specific CD8+ T cell responses may be involved (15–18). Myelin-specific CD8+ T cells have also been reported to exhibit a more activated, memory phenotype in MS patients compared with healthy controls (19). These observations point to a functional contribution of CD8+ T cells in MS; however, it is unclear whether CD8+ T cells exert pathogenic or regulatory effects. One study investigating myelin-specific CD8+ T cells in patients with MS detected expression of both pro- and antiinflammatory immune mediators within this population, suggesting the presence of both pathogenic and regulatory CD8+ T cells (20). Furthermore, distinct HLA-A alleles have been associated with both increased and decreased susceptibility to MS (21), a finding that has been reproduced in humanized mouse models (22). CD8+ T cells isolated from patients with MS have been reported to suppress the activity of myelin-specific CD4+ T cells, and relapses have been correlated with a reduction in the suppressive function of CD8+ T cells, consistent with a regulatory function (23, 24). However, oth-

er evidence from MS patients supports a pathogenic role for CD8⁺ T cells. In MS brain tissues, CD8⁺ T cells with polarized cytotoxic granules are located in close proximity to demyelinated axons (25), and the number of CD8⁺ T cells correlates with the extent of axon damage (26). In mice, CD8⁺ T cells specific for CNS antigens can exacerbate CD4⁺ T cell–mediated EAE (27) and can also induce CNS autoimmunity on their own (22, 28–33). Thus, similarly to pathogenic and regulatory CD4⁺ T cells, different types of CD8⁺ T cells may exert different functions in MS.

To investigate the potential roles of CD8⁺ T cells in CNS autoimmunity, we previously generated T cell receptor–transgenic (TCR-transgenic) mice specific for an epitope of myelin basic protein (MBP) presented by the MHC class I molecule H-2K^k (MBP/K^k), termed "8.8" mice (34). Infection of these mice with a recombinant vaccinia virus expressing MBP triggered CNS autoimmunity initiated by the 8.8 CD8⁺ T cells (35). However, in light of the importance of CD4⁺ T cells in MS, we sought to develop a model in which we could investigate whether naive myelin-specific CD8⁺ T cells recruited to the CNS during EAE initiated by CD4⁺ T cells (CD4-initiated EAE) influenced the disease. To validate this approach, we showed in earlier studies that the MBP/K^k ligand is presented by a small population of oligodendrocytes and a larger population of myeloid cells during CD4-initiated EAE (35). This observation indicated that 8.8 CD8⁺ T cells could potentially engage in cognate interactions with antigen-presenting cells (APCs) in this inflammatory milieu if they infiltrated the CNS. Here, we investigated whether naive 8.8 CD8⁺ T cells injected into the periphery of WT mice infiltrated the CNS and influenced CD4-initiated EAE. Surprisingly, we found that 8.8 CD8⁺ T cells exacerbated atypical but not classic EAE. The increase in incidence and severity of atypical EAE that occurred upon recruitment of 8.8 CD8⁺ T cells was associated with increased chemokine and cytokine expression, as well as an increase in the number of parenchymal lesions and tissue injury, in the brain and not the spinal cord. Although the 8.8 CD8⁺ T cells infiltrated both the brain and spinal cord during CD4-initiated EAE, they accumulated only in the brain. Consistent with this, a higher frequency of monocytes and monocyte-derived cells (MdCs) presenting MBP/K^k was detected in the brain compared with the spinal cord. Importantly, recruitment of 8.8 CD8⁺ T cells to the CNS enhanced reactive oxygen species (ROS) production in monocytes and MdCs in the brain but not spinal cord via a Fas ligand–dependent (FasL-dependent) mechanism. These findings revealed a proinflammatory mechanism by which myelin-specific CD8⁺ T cells promote brain versus spinal cord inflammation in EAE.

Results

8.8 CD8⁺ T cells exacerbate atypical but not classic CD4-initiated EAE. To determine whether naive 8.8 CD8⁺ T cells were recruited to the CNS and influenced the disease course of CD4-initiated EAE, we first introduced either 8.8 or WT (control) CD8⁺ T cells into the periphery of WT mice. EAE was then induced by adoptive transfer of CD4⁺ T cells specific for an epitope of myelin oligodendrocyte glycoprotein (MOG$_{97–114}$). We used CD4⁺ T cells from mice immunized with MOG that were skewed toward a Th17 phenotype in vitro (referred to as donor CD4⁺ T cells), as we previously showed that Th17-skewed CD4⁺ T cells promote brain as well as spinal cord

inflammation (7). Therefore, this approach allowed us to monitor exacerbating or ameliorating effects of 8.8 CD8⁺ T cells on both classic and atypical EAE. Mice that received only naive 8.8 CD8⁺ T cells without donor CD4⁺ T cells exhibited no clinical signs (Figure 1A). WT mice with CD4-initiated EAE that had received either naive 8.8 CD8⁺ T cells (referred to as CD4-initiated/CD8$_{8.8}$) or WT CD8⁺ T cells (referred to as CD4-initiated/CD8$_{WT}$) developed classic EAE with comparable incidence and severity (Figure 1, A and B). However, both the incidence and severity of atypical EAE were significantly higher in mice with CD4-initiated/CD8$_{8.8}$ EAE compared with mice with CD4-initiated/CD8$_{WT}$ EAE (Figure 1, C and D). These data suggest that recruitment of 8.8 CD8⁺ T cells specifically enhances inflammation in the brain but not the spinal cord.

Tissue injury was assessed histologically in mice with CD4-initiated/CD8$_{8.8}$ and CD4-initiated/CD8$_{WT}$ EAE by determination of the extent of inflammatory cell accumulation and associated cell death seen in brain and spinal cord sections. Consistent with the increased severity of atypical clinical signs in mice with CD4-initiated/CD8$_{8.8}$ EAE, tissue injury was more severe in the brains of these mice compared with the brains of mice with CD4-initiated/CD8$_{WT}$ EAE (Figure 1E). In addition, the lesions within each section were characterized as involving the meninges only, meninges with extension into submeningeal tissue, or parenchymal blood vessels and adjacent tissue. While all mice in both groups exhibited lesions involving the meningeal and submeningeal regions in the brain and spinal cord (data not shown), more lesions centered on parenchymal blood vessels were observed in the brains of mice with CD4-initiated/CD8$_{8.8}$ EAE compared with those with CD4-initiated/CD8$_{WT}$ EAE (Figure 1F and Supplemental Figure 1, A–C; supplemental material available online with this article; https://doi.org/10.1172/JCI132531DS1). No differences in histology score or the frequency of parenchymal lesions were observed in the spinal cord (Figure 1, E and F). Together, these data suggest that recruitment of 8.8 CD8⁺ T cells during CD4-initiated EAE enhances tissue injury in the brain, especially around parenchymal blood vessels.

8.8 CD8⁺ T cells accumulate and acquire a more activated phenotype in the brain compared with the spinal cord. As the introduction of 8.8 CD8⁺ T cells had a greater clinical and histological impact on the brain compared with the spinal cord, we hypothesized that the recruitment and/or activation of the 8.8 CD8⁺ T cells would differ between these 2 regions. We first analyzed the numbers of 8.8 CD8⁺ T cells infiltrating the brain and spinal cord on days 4 and 5 (preclinical), day 6 (on or just prior to onset), and day 7 (a time point by which 80% of the mice developed either classic or atypical EAE) after CD4⁺ T cell transfer by flow cytometry (gating strategy shown in Supplemental Figure 2A). Interestingly, although 8.8 CD8⁺ T cells entered the spinal cord 1 day earlier than the brain (day 4 vs. day 5), the number of 8.8 CD8⁺ T cells increased over time only in the brain (Figure 2A). This phenomenon was not due to overall inflammation increasing only in the brain, as the numbers of CD45^{hi} inflammatory cells and donor CD4⁺ T cells accumulated over time in both the brain and spinal cord (Figure 2, B and C). We next compared the expression of activation markers on 8.8 CD8⁺ T cells in the brain versus spinal cord during CD4-initiated EAE. Because recovery of 8.8 CD8⁺ T cells from the CNS tissue is low, consistent with the reported low efficiency of isolating acti-
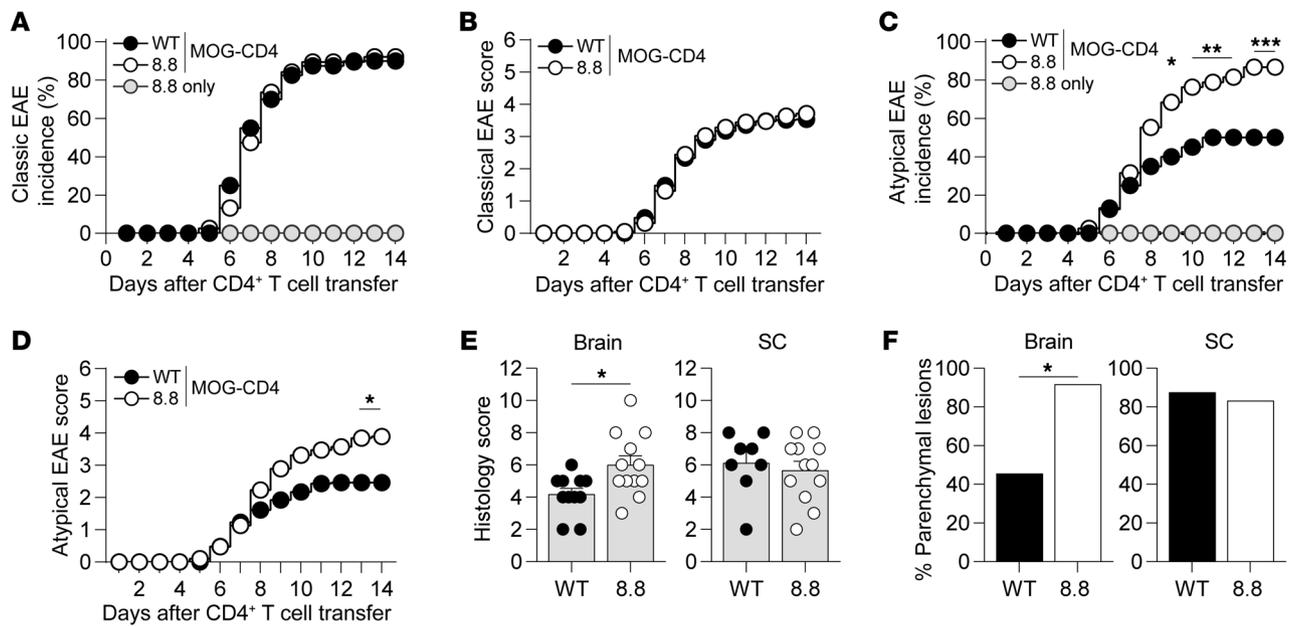
Figure 1. 8.8 CD8+ T cells exacerbate atypical but not classic CD4-initiated EAE. EAE was induced by transfer of MOG-specific CD4+ T cells into WT mice that received either WT or 8.8 CD8+ T cells 1 day earlier. Control mice that received 8.8 CD8+ T cells and no CD4+ T cells are designated "8.8 only." (**A**) Incidence of classic EAE among all mice is shown for each indicated group. (**B**) Classic EAE scores (mean ± SEM) are shown for mice that developed EAE. (**C**) Incidence of atypical EAE among all mice is shown for each indicated group. (**D**) Atypical EAE scores (mean ± SEM) are shown for mice that developed EAE. (**E**) Histology scores (assigned as described in Methods, mean + SEM) are shown for brain and spinal cord (SC) tissues harvested 7 days after CD4+ T cell transfer. Tissues that contained at least 1 lesion in the corresponding region were included in the analyses. (**F**) The percentage of mice evaluated in **E** that exhibited parenchymal blood vessel–associated lesions is shown. Representative brain sections for **E** and **F** are shown in Supplemental Figure 1. (**A**–**D**) Data are compiled from 8 independent experiments; $n = 40$ for EAE-induced recipients of WT CD8+ T cells; $n = 38$ for EAE-induced recipients of 8.8 T cells; $n = 5$ for mice that received only 8.8 T cells. (**E** and **F**) Data are from 2 independent experiments; $n = 12$ mice per group. Statistical significance was determined using Fisher's exact test (**A**, **C**, and **F**) or Mann-Whitney U test (**B**, **D**, and **E**). $*P < 0.05$, $**P < 0.01$, $***P < 0.001$.

vated CD8+ T cells from tissues (36), we induced disease by transferring CD4+ T cells directly into intact TCR-transgenic 8.8 mice in order to increase the number of 8.8 CD8+ T cells available for analyses by flow cytometry. We confirmed that the incidence of atypical (Supplemental Figure 2B) but not classic (data not shown) EAE was also significantly higher in intact 8.8 compared with WT recipients. On day 7 after CD4+ T cell transfer, 8.8 CD8+ T cells exhibited a CD44hiCD62Llo activated phenotype in the brain and spinal cord but not the spleen (Supplemental Figure 2C), suggesting that 8.8 CD8+ T cells are activated within the CNS. Interestingly, the frequency of 8.8 CD8+ T cells exhibiting a CD44hiCD62Llo activated phenotype was higher in the brain compared with the spinal cord, and the frequency of 8.8 CD8+ T cells exhibiting a CD44loCD62Lhi naive phenotype was lower in the brain compared with the spinal cord (Figure 2D). These data suggest that 8.8 CD8+ T cells preferentially accumulate and appear more activated within the brain compared with the spinal cord.

The preferential accumulation of 8.8 CD8+ T cells in the brain could result from differences in their recruitment from the periphery, proliferation, or survival in the brain versus the spinal cord. We first compared 8.8 CD8+ T cell death and proliferation in the brain and spinal cord 7 days after CD4+ T cell transfer into intact 8.8 mice. In contrast to the minimal 8.8 CD8+ T cell death seen in the spleen, more cell death was observed in the CNS tissues (Supplemental Figure 3A). A significantly higher frequency of dead 8.8 CD8+ T cells was observed in the spinal cord (Supplemental Figure 3A); however, we also observed a higher frequency of dead donor

CD4+ T cells in the spinal cord compared with the brain (Supplemental Figure 3B). This overall increased frequency of T cell death suggests that T cell death within the spinal cord may be a general phenomenon and not specific to 8.8 CD8+ T cells. While we cannot exclude the possibility that enhanced cell death accounts for the lack of 8.8 CD8+ T cell accumulation in the spinal cord, the percentage of cell death in the spinal cord exhibited by donor CD4+ T cells was similar to that shown by 8.8 CD8+ T cells, yet these CD4+ T cells still accumulated over time in the spinal cord (Figure 2C). Proliferation of 8.8 CD8+ T cells was not seen in the spleen, and similar frequencies of proliferating 8.8 CD8+ T cells were observed in the brain and spinal cord (Supplemental Figure 3C). To compare recruitment of 8.8 CD8+ T cells from the periphery to the brain and spinal cord, we administered either a spingosine-1-phosphate receptor modulator (FTY720) that retains lymphocytes in peripheral lymphoid tissues or vehicle to mice with CD4-initiated/CD8$_{8.8}$ EAE on day 6 and analyzed 8.8 CD8+ T cell numbers in each CNS tissue 1 day later. If there was greater recruitment of 8.8 CD8+ T cells to the brain compared with the spinal cord, a larger fold decrease in 8.8 CD8+ T cell number in the brain compared with the spinal cord should be observed in treated versus untreated mice. However, significantly fewer 8.8 CD8+ T cells were observed in both the brain and spinal cord following FTY720 administration (Supplemental Figure 3D), and the fold decrease in the mean numbers of 8.8 CD8+ T cells was not higher in the brain (5.6-fold decrease) compared with the spinal cord (11.8-fold decrease). These data are not consistent with increased recruitment of 8.8 CD8+ T cells from the periphery to the
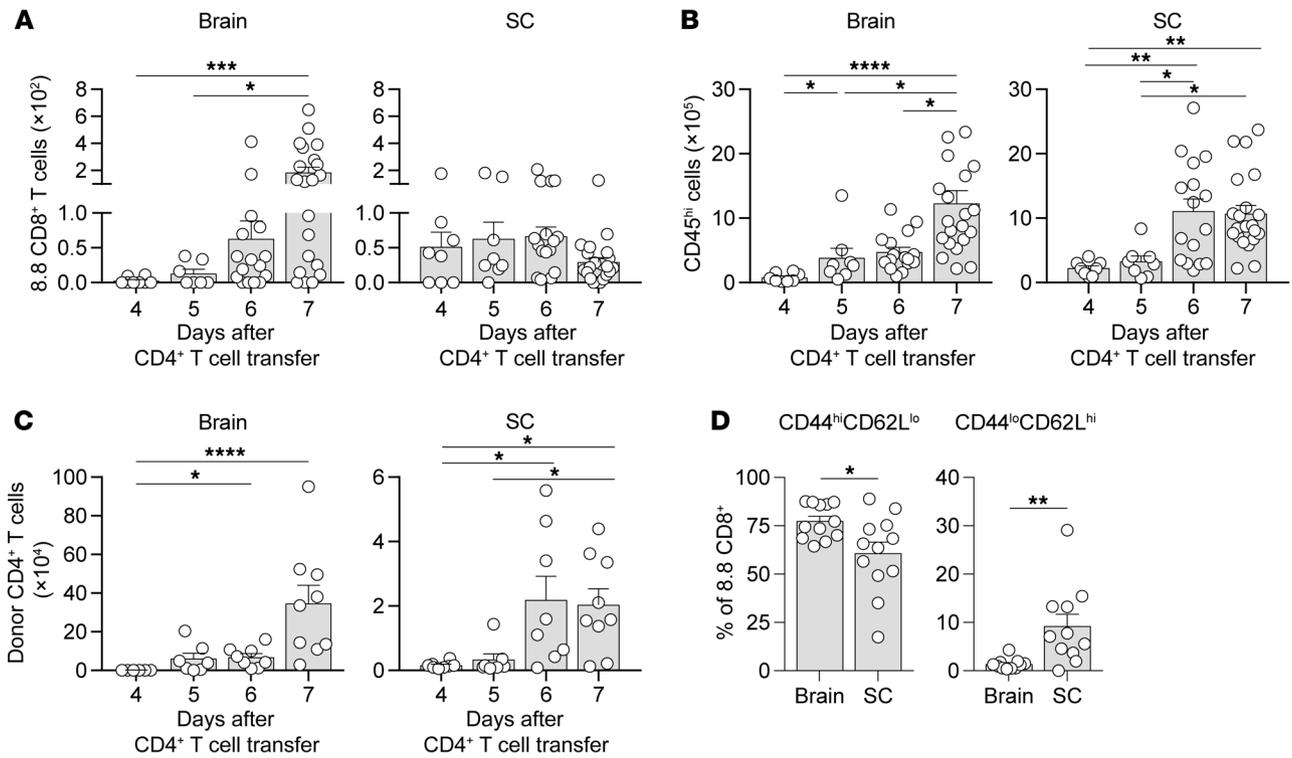
Figure 2. 8.8 CD8+ T cells accumulate and acquire a more activated phenotype in the brain compared with spinal cord. (A–C) EAE was induced by transfer of CD45.1.2+ MOG-specific CD4+ T cells into CD45.1.1+ mice that had received CD45.2.2+ 8.8 CD8+ T cells 1 day earlier. The numbers of 8.8 CD8+ T cells (A), CD45hi inflammatory cells (B), and donor CD4+ T cells (C) were determined for the brain and spinal cord (SC) by flow cytometry on the indicated days after CD4+ T cell transfer ($n \geq 8$ for each day). (D) EAE was induced by transfer of CD45.1.1+ MOG-specific CD4+ T cells into CD45.2.2+ WT or 8.8 intact mice ($n = 12$). Mononuclear cells were isolated from the brain and spinal cord 7 days after CD4+ T cell transfer and analyzed by flow cytometry. The percentage of activated (CD44hiCD62Llo) and naive (CD44loCD62Lhi) 8.8 CD8+ T cells is shown. Gating strategies are shown in Supplemental Figure 2. Graphs show mean + SEM (1 symbol per mouse) and are compiled from at least 2 independent experiments. Statistical significance was determined using Kruskal-Wallis with Dunn's post-test (A–C) or Mann-Whitney U test (D). *$P < 0.05$, **$P < 0.01$, ***$P < 0.001$, ****$P < 0.0001$.

brain versus the spinal cord. Collectively, these data suggest that the preferential increase of 8.8 CD8+ T cells in the brain is independent of differences in recruitment from the periphery, proliferation, or cell death between the brain and spinal cord.

Recruitment of 8.8 CD8+ T cells to the brain is associated with enhanced expression of inflammatory mediators and increased numbers of monocytes, MdCs, and donor CD4+ T cells. We hypothesized that the exacerbation of atypical but not classic EAE may correlate with increased expression of proinflammatory mediators in the brains but not spinal cords of mice with CD4-initiated/CD8₈.₈ compared with CD4-initiated/CD8ₐₜ EAE. To test this hypothesis, we analyzed gene expression of a panel of inflammatory mediators in CNS tissues harvested from mice 6 days after CD4+ T cell transfer and determined their fold induction relative to irradiated healthy control mice that received no T cells. Multiple chemokines involved in myeloid and T cell recruitment exhibited a significantly greater fold induction in the brains of mice with CD4-initiated/CD8₈.₈ compared with CD4-initiated/CD8ₐₜ EAE (Figure 3A). There was a trend toward increased expression of genes encoding CCL2, CCL5, CCL6, CCL9, and CCL11 in the spinal cord of mice with CD4-initiated/CD8₈.₈ versus CD4-initiated/CD8ₐₜ EAE; however, these data did not reach statistical significance (Figure 3A). Cytokines implicated in EAE pathogenesis were also induced to a greater extent in the brains of CD4-initiated/CD8₈.₈ compared

with CD4-initiated/CD8ₐₜ EAE mice, including genes encoding IL-17, GM-CSF, TNF-α, IL-6, and IL-1β (Figure 3B). IFN-γ also demonstrated a trend toward increased expression in the brains of mice with CD4-initiated/CD8₈.₈ EAE (Figure 3B). No differences in induction of these cytokines were seen in the spinal cord (Figure 3B). Both groups of mice exhibited similar fold changes in expression of genes encoding CCL22, CCL24, IL-10, IL-12p35, IL-23p19, IFN-β, and TGF-β in the brain and spinal cord (data not shown). These data demonstrate that infiltration of 8.8 CD8+ T cells in the brain, and to a lesser extent the spinal cord, is associated with enhanced production of soluble mediators that recruit inflammatory cells and enhance their pathogenic activity.

To determine whether the enhanced expression of chemokines and cytokines observed when 8.8 CD8+ T cells infiltrate the brain influenced the inflammatory infiltrate, we compared the numbers of monocytes, MdCs, neutrophils, microglia, and donor CD4+ T cells in mice with CD4-initiated/CD8₈.₈ and CD4-initiated/CD8ₐₜ EAE (gating strategy shown in Supplemental Figure 4A). The number of monocytes was significantly higher in the brains of mice with CD4-initiated/CD8₈.₈ compared with CD4-initiated/CD8ₐₜ EAE on days 5 and 7 after CD4+ T cell transfer, and the number of MdCs trended higher on day 5 and was significantly higher on day 7 (Figure 3C). The numbers did not differ for either cell type at either time point in the spinal cord (Figure 3C). Microg-
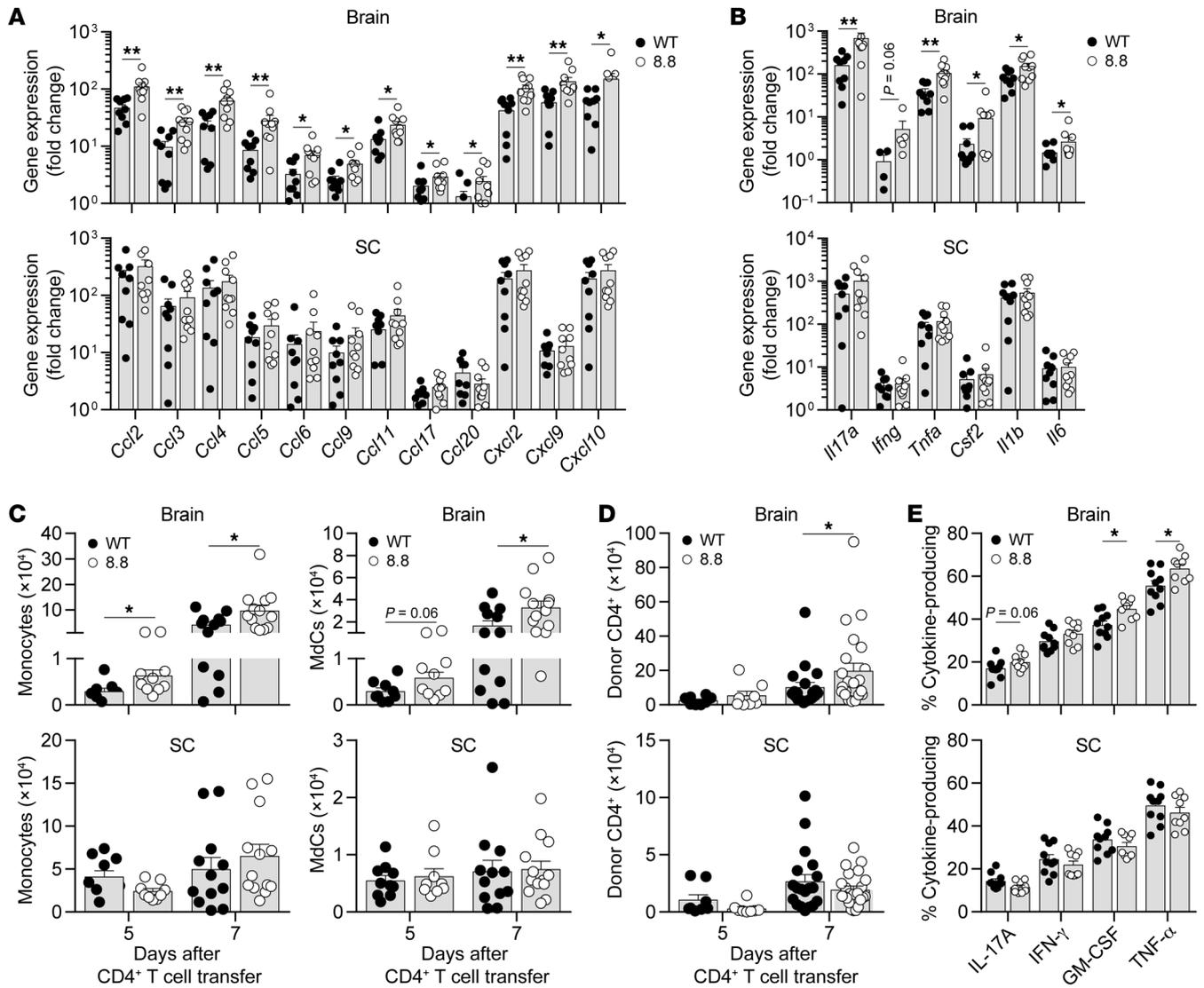
Figure 3. Recruitment of 8.8 CD8+ T cells enhances chemokine and cytokine gene expression as well as the numbers of donor CD4+ T cells, MdCs, and monocytes in the brain. EAE was induced by transfer of Thy1.1+ MOG-specific CD4+ T cells into Thy1.2+ WT mice that had received Thy1.2+ WT or 8.8 CD8+ T cells. (**A** and **B**) Brain and spinal cord (SC) tissues were harvested 6 days after CD4+ T cell transfer (WT, $n = 9$; 8.8, $n = 10$). Chemokine (**A**) and cytokine (**B**) gene expression were analyzed directly ex vivo by quantitative PCR. All data were normalized to GAPDH. The fold change was calculated relative to gene expression values in irradiated healthy control mice ($n = 2$). (**C**) The numbers of CD45hiCD11b+Ly6ChiMHCII− monocytes and CD45hiCD11b+Ly6C+/−MHCII+ MdCs were determined on days 5 (WT, $n = 9$; 8.8, $n = 10$) and 7 (WT, $n = 12$; 8.8, $n = 13$) after CD4+ T cell transfer for the brain and spinal cord by flow cytometry. (**D**) The number of Thy1.1+ donor CD4+ T cells was determined on days 5 ($n = 8$ per group) and 7 (WT, $n = 19$; 8.8, $n = 23$) after CD4+ T cell transfer for the brain and spinal cord by flow cytometry. (**E**) Brain and spinal cord mononuclear cells isolated from WT ($n = 10$) and 8.8 ($n = 9$) recipients on day 7 after CD4+ T cell transfer were stimulated with MOG$_{97-114}$ before intracellular cytokine staining. Percentages of Thy1.1+ donor CD4+ T cells producing the indicated cytokines are shown. Gating strategies for **C**–**E** are shown in Supplemental Figure 4. Graphs show mean + SEM (1 mouse per symbol) and are compiled from at least 2 independent experiments. Statistical significance was determined using a Mann-Whitney U test. *$P < 0.05$, **$P < 0.01$.

lia and neutrophil numbers were not significantly different in the brain or spinal cord at either time point (Supplemental Figure 4B). Similar numbers of donor CD4+ T cells were observed in the brains of mice in both groups on day 5; however, a significantly higher number of donor CD4+ T cells was found in the brains of mice with CD4-initiated/CD8$_{8.8}$ compared with CD4-initiated/CD8$_{WT}$ EAE on day 7 (Figure 3D). No differences in donor CD4+ T cell numbers were seen between groups at either time point in the spinal cord (Figure 3D) or spleen (data not shown). The cytokine production by donor CD4+ T cells was also analyzed on day 7 after CD4+ T

cell transfer (gating strategy shown in Supplemental Figure 4C). A significantly higher percentage of donor CD4+ T cells produced TNF-α and GM-CSF in the brain but not spinal cord of CD4-initiated/CD8$_{8.8}$ mice (Figure 3E), with similar trends observed for IL-17 and IFN-γ. Together, these data suggest that 8.8 CD8+ T cells enhance the recruitment and differentiation of monocytes followed by increased recruitment of pathogenic donor CD4+ T cells specifically to the brain and not the spinal cord.

8.8 CD8+ T cell effector phenotype differs in the brain versus the spinal cord. We analyzed production of effector cytokines by CD8+ T
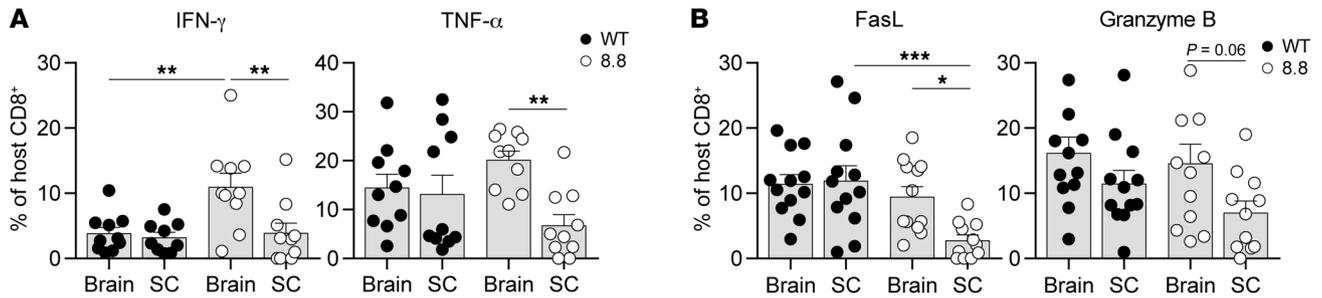
Figure 4. 8.8 CD8+ T cells exhibit functional differences in the brain versus the spinal cord. EAE was induced by transfer of CD45.1.1+ MOG-specific CD4+ T cells into CD45.2.2+ WT or 8.8 intact mice. Mononuclear cells were isolated from brain and spinal cord 7 days after CD4+ T cell transfer and analyzed by flow cytometry. (**A**) The percentage of cytokine-producing WT and 8.8 CD8+ T cells following culture only with GolgiPlug is shown (*n* = 10 per group). (**B**) The percentage of FasL+ and granzyme B+ WT and 8.8 CD8+ T cells is shown (*n* = 12 per group). Gating strategies for **A** and **B** are shown in Supplemental Figure 5. Graphs show mean + SEM (1 symbol per mouse) and are compiled from 2 independent experiments. Statistical significance was determined using 2-way ANOVA with Šidák's post-test. *$P < 0.05$, **$P < 0.01$, ***$P < 0.001$.

cells isolated from intact 8.8 or WT mice directly ex vivo 7 days after CD4+ T cell transfer. As expected, 8.8 CD8+ T cells from the spleen produced no cytokines (Supplemental Figure 5A). In contrast, 8.8 CD8+ T cells isolated from the brain and spinal cord produced IFN-γ and TNF-α but not GM-CSF or IL-17 (Supplemental Figure 5A). Interestingly, the frequency of IFN-γ– and TNF-α–producing CD8+ T cells was significantly higher in the brain compared with the spinal cord in 8.8 mice (Figure 4A). This enrichment of cytokine-producing CD8+ T cells in the brain versus the spinal cord was specific to 8.8 mice, as CD8+ T cells isolated from the CNS of WT mice showed similar frequencies of IFN-γ– and TNF-α–producing CD8+ T cells in the brain and spinal cord (Figure 4A). Importantly, the frequency of IFN-γ–producing CD8+ T cells was significantly higher in the brains of 8.8 compared with WT mice (Figure 4A), indicating that this response was antigen-specific. The frequency of TNF-α–producing CD8+ T cells also trended higher in the brains of 8.8 compared with WT mice (Figure 4A). FasL- and granzyme B–expressing CD8+ T cells were also seen in the brain and spinal cord but not the spleen of 8.8 mice (Supplemental Figure 5B). As observed for cytokine-producing 8.8 CD8+ T cells, the frequency of FasL-expressing 8.8 CD8+ T cells was significantly lower in the spinal cord compared with the brain, and the frequency of granzyme B–expressing 8.8 CD8+ T cells also trended lower in the spinal cord (Figure 4B). FasL- and granzyme B–expressing CD8+ T cells were also observed in the CNS of WT mice; however, the frequencies of these cells did not differ between the brain and spinal cord and were comparable to the frequencies seen in the brains of 8.8 mice (Figure 4B). Together, these data indicate that expression of FasL and granzyme B is likely caused by bystander activation within the inflamed CNS, but the higher frequency of IFN-γ–producing and possibly TNF-α–producing 8.8 compared with WT CD8+ T cells in the brain suggests an antigen-specific response. These analyses also revealed a striking difference between 8.8 and WT CD8+ T cells infiltrating the CNS in that only 8.8 CD8+ T cells exhibited a lower frequency of cells expressing these activation markers in the spinal cord versus the brain.

Increased presentation of MBP/K^k in the brain versus spinal cord is associated with enhanced activation of myeloid cells in the brain. As the frequencies of 8.8 CD8+ T cells expressing markers of activation and effector function were all significantly higher in the

brain than the spinal cord, we hypothesized that 8.8 CD8+ T cells encounter their ligand more frequently in the brain compared with the spinal cord. To test this hypothesis, we analyzed the frequency of APCs presenting MBP/K^k in the brain and spinal cord in mice with CD4-initiated EAE using an antibody specific for the MBP/K^k ligand (35). MdCs and monocytes were identified as the predominant myeloid cells presenting MBP/K^k in both the brain and spinal cord (Figure 5A and Supplemental Figure 6A). Although a small population of microglia also presented MBP/K^k (Figure 5A and Supplemental Figure 6A), we previously showed that this population does not elicit 8.8 CD8+ T cell functional responses (35). Importantly, the frequency of MdCs and monocytes expressing MBP/K^k was significantly higher in the brain compared with the spinal cord (Figure 5A), consistent with the notion that 8.8 CD8+ T cells encounter APCs presenting their cognate antigen more frequently in the brain compared with the spinal cord.

We next determined whether the activity of the MdCs and monocytes was influenced by the infiltration of 8.8 CD8+ T cells by analyzing their production of ROS, which are implicated in mediating demyelination, oligodendrocyte cell death, and axon degeneration in MS and EAE (37–40). On day 7, MdCs and monocytes in the brain but not spinal cord produced significantly more ROS in mice with CD4-initiated/CD8$_{8.8}$ EAE compared with mice with CD4-initiated/CD8$_{WT}$ EAE (Figure 5, B and C). In contrast, no differences were observed between the 2 groups of mice in ROS production by microglia and neutrophils in either the brain or spinal cord, consistent with a lack of MBP/K^k expression on these cell types (Supplemental Figure 6, B and C). The observations that MdCs and monocytes are the predominant myeloid cells in the CNS that present MBP/K^k and are the only cell types whose ROS production was affected by the infiltration of 8.8 CD8+ T cells are consistent with the notion that cognate interactions between these cell types enhance proinflammatory responses. Furthermore, our data suggest that these interactions should occur more frequently in the brain compared with the spinal cord, as the frequency of MBP/K^k+ MdCs and monocytes is significantly lower in the spinal cord and their ROS production is not affected by infiltration of 8.8 CD8+ T cells.

FasL signaling mediated by 8.8 CD8+ T cells is required to exacerbate atypical EAE and enhance myeloid cell ROS production. To
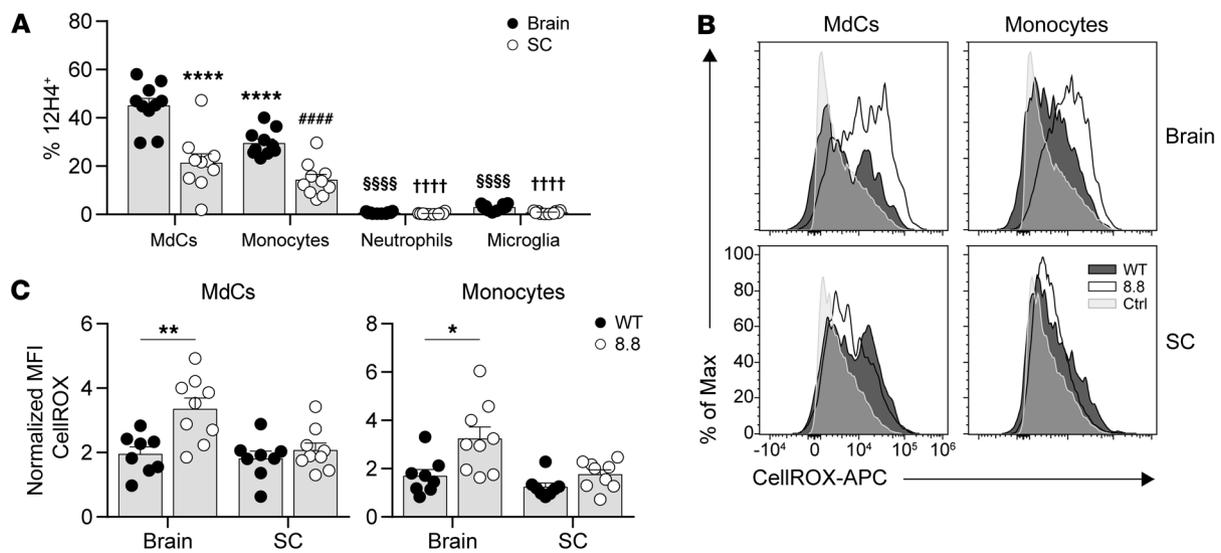
Figure 5. Increased presentation of MBP/K^k in the brain versus spinal cord is associated with enhanced activation of myeloid cells in the brain. (**A**) EAE was induced by transfer of MOG-specific CD4$^+$ T cells into WT mice ($n = 10$). Mononuclear cells were isolated from the brains and spinal cords (SC) of mice on day 7 after CD4 T cell transfer. Percentages of 12H4$^+$ cells among MdCs, monocytes, neutrophils, and microglia are shown. Gating strategy is shown in Supplemental Figure 6A. ****$P < 0.0001$ vs. MdCs isolated from the brain; ####$P < 0.0001$ vs. monocytes isolated from the brain; §§§§$P < 0.0001$ vs. both MdCs and monocytes from the brain; ††††$P < 0.0001$ vs. both MdCs and monocytes from the spinal cord. (**B** and **C**) EAE was induced by transfer of MOG-specific CD4$^+$ T cells into WT mice that had received WT ($n = 8$) or 8.8 ($n = 9$) CD8$^+$ T cells. Representative flow cytometry plots (**B**) and normalized MFIs (medians) (**C**) of ROS production (using CellROX) gated on MdCs and monocytes isolated from brains and spinal cords of mice on day 7 after CD4$^+$ T cell transfer. MFIs are normalized to the MFI for T cell CellROX staining (Ctrl). (**A** and **C**) Graphs show mean + SEM (1 symbol per mouse) and are compiled from 2 independent experiments. Statistical significance was determined using a 2-way ANOVA with Šidák's post-test (**A**) or Mann-Whitney U test (**C**). *$P < 0.05$, **$P < 0.01$.

define the effector functions required for 8.8 CD8$^+$ T cells to exacerbate brain inflammation in CD4-initiated EAE, we introduced CD8$^+$ T cells isolated from either WT mice, 8.8 mice, or 8.8 mice on an IFN-γ–deficient (IFN-γ$^{-/-}$), perforin-deficient (Pfp$^{-/-}$), TNF-α–deficient (TNF-α$^{-/-}$), or FasL-deficient (FasL^{gld}) background into WT mice before transfer of MOG-specific CD4$^+$ T cells. All groups of mice exhibited similar classic EAE incidence (data not shown). The incidence of atypical EAE seen in the groups of mice that received 8.8, IFN-γ$^{-/-}$ 8.8, Pfp$^{-/-}$ 8.8, or TNF-α$^{-/-}$ 8.8 CD8$^+$ T cells was similar and was significantly higher in comparison with mice that received WT CD8$^+$ T cells (Figure 6, A–C). Strikingly, FasL^{gld} 8.8 CD8$^+$ T cells did not exacerbate atypical EAE, as the incidence of atypical EAE in mice that received FasL^{gld} 8.8 CD8$^+$ T cells was similar to that in mice that received WT CD8$^+$ T cells, and was significantly lower than that seen in 8.8 CD8$^+$ T cell recipients (Figure 6D). These data demonstrate that FasL signaling, and not IFN-γ, perforin, or TNF-α production, is required for 8.8 CD8$^+$ T cells to exacerbate atypical CD4-initiated EAE.

We then investigated whether FasL expression by 8.8 CD8$^+$ T cells was required for the enhanced ROS production by MdCs and monocytes, as Fas signaling has been shown to activate these cell types to produce proinflammatory mediators (41–44). Importantly, MdCs in the brains of mice that received FasL^{gld} 8.8 CD8$^+$ T cells failed to upregulate ROS production (Figure 6, E and F). Monocytes in the brains of mice that received FasL^{gld} 8.8 CD8$^+$ T cells also did not upregulate ROS production, although the comparison with mice that received 8.8 CD8$^+$ T cells did not reach statistical significance (Figure 6, E and F). These data indicate that 8.8 CD8$^+$ T cells activate MdCs and likely monocytes via a FasL-mediated mechanism to produce ROS in the brain.

Discussion

In this study, we investigated how naive myelin-specific CD8$^+$ T cells recruited to the CNS during the initial stages of CD4-initiated EAE influenced disease. Strikingly, we found that recruitment of 8.8 CD8$^+$ T cells exacerbated atypical but not classic EAE, reflecting an increase in both tissue injury and number of parenchymal blood vessel–associated lesions in the brain compared with the spinal cord. Although 8.8 CD8$^+$ T cells were recruited to and activated within both the brain and spinal cord, 8.8 CD8$^+$ T cells accumulated over time only in the brain, and a higher frequency of 8.8 CD8$^+$ T cells exhibited an activated phenotype in the brain compared with the spinal cord. Recruitment of 8.8 CD8$^+$ T cells resulted in enhanced ROS production by monocytes and MdCs in the brain that required FasL expression by 8.8 CD8$^+$ T cells. These results identified a novel mechanism by which myelin-specific CD8$^+$ T cells enhance inflammatory responses specifically in the brain during CD4-intiated EAE.

Our previous work demonstrated that both myeloid cells and oligodendrocytes present MBP/K^k in the CNS during EAE initiated by MOG-specific CD4$^+$ T cells (35), suggesting the potential for determinant spreading between myelin-specific CD4$^+$ and CD8$^+$ T cells. In those experiments, cells were pooled from brain and spinal cord tissue and analyzed for expression of MBP/K^k. Here we defined the MBP/K^{k+} myeloid cells as monocytes and MdCs. We found that the frequency of these MBP/K^{k+} APCs was higher in the brain compared with the spinal cord, revealing another difference in inflammatory responses between the brain and spinal cord in EAE (6). Consistent with increased antigen presentation in the brain, IFN-γ production by 8.8 CD8$^+$ T cells appeared to be antigen-specific in the brain, as the frequency of IFN-γ$^+$ 8.8 CD8$^+$
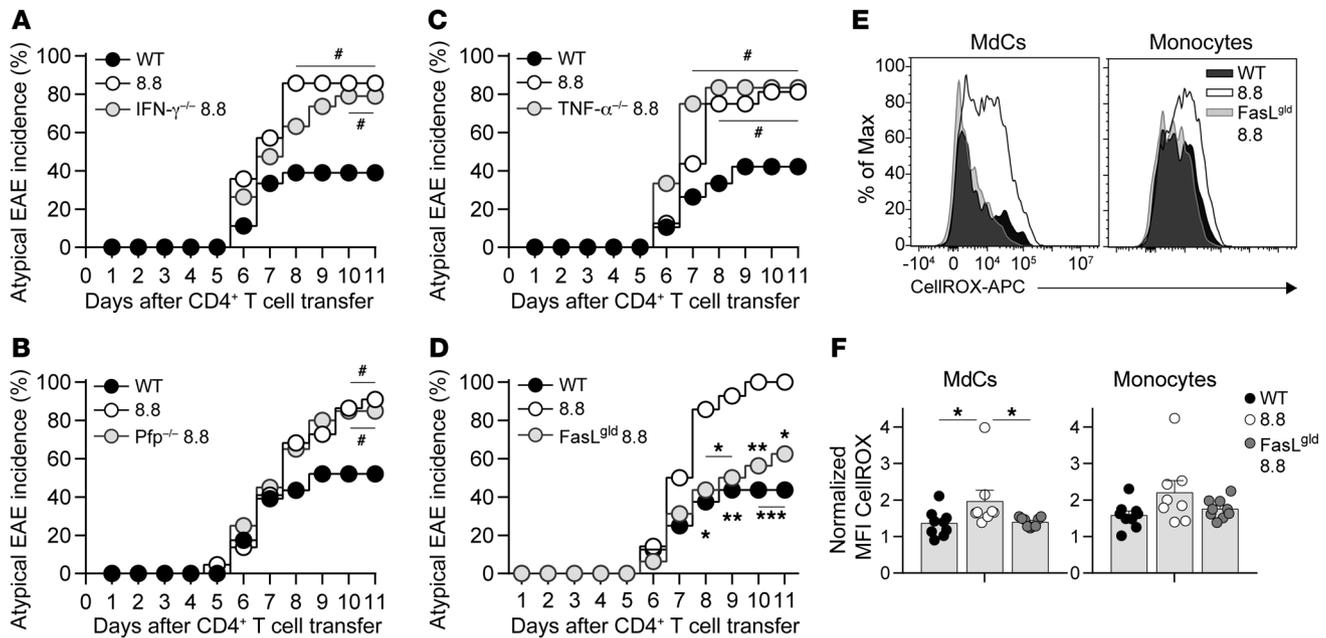
Figure 6. Atypical EAE is exacerbated by 8.8 CD8+ T cells via a FasL-dependent mechanism. (**A–D**) EAE was induced by transfer of MOG-specific CD4+ T cells into WT mice that had received WT (n = 18), 8.8 (n = 14), or IFN-γ–deficient (IFN-γ−/−) 8.8 (n = 19) CD8+ T cells (**A**); WT (n = 23), 8.8 (n = 22), or perforin-deficient (Pfp−/−) 8.8 (n = 20) CD8+ T cells (**B**); WT (n = 19), 8.8 (n = 16), or TNF-α–deficient (TNF-α−/−) 8.8 (n = 12) CD8+ T cells (**C**); and WT (n = 16), 8.8 (n = 14), or FasL-deficient (FasLgld) 8.8 (n = 16) CD8+ T cells (**D**). The percentage of mice exhibiting atypical EAE is shown for each group. (**E** and **F**) EAE was induced by transfer of MOG-specific CD4+ T cells into WT mice that had received WT (n = 9), 8.8 (n = 8), or FasLgld (n = 9) CD8+ T cells. Representative flow cytometry plot (**E**) and normalized MFIs (medians) (**F**) of ROS staining (using CellROX) gated on MdCs and monocytes within mononuclear cells isolated from the brains of mice on day 7 after CD4 transfer. MFIs are normalized to the MFI for T cell CellROX staining. Graphs show mean + SEM (1 symbol per mouse) and are compiled from 2 independent experiments. (**A–D**) Data in each panel are compiled from at least 3 independent experiments. Statistical significance was determined using Fisher's exact test (**A–D**) or Mann-Whitney U test (**F**). #P < 0.05 vs. mice that received WT CD8+ T cells; *P < 0.05, **P < 0.01, ***P < 0.001 vs. mice that received 8.8 CD8+ T cells.

T cells was significantly higher than the frequency of IFN-γ+ WT CD8+ T cells in this region. A similar trend was observed for TNF-α production. Cytokine production by 8.8 CD8+ T cells in the spinal cord did not appear to be antigen-specific, as the frequencies of cytokine-producing T cells were similar for 8.8 and WT CD8+ T cells in this region. These data suggest that the increased frequency of MBP/Kk+ APCs in the brain allows 8.8 CD8+ T cells to engage in cognate interactions with monocytes/MdCs more frequently in the brain than the spinal cord. However, IFN-γ production by 8.8 CD8+ T cells was not required for the exacerbation of atypical EAE. This finding may reflect the fact that the MOG-specific CD4+ T cells infiltrating the CNS also produce IFN-γ in the brain and the number of donor CD4+ T cells is larger compared with the number of 8.8 CD8+ T cells recruited to the CNS during the initial days leading up to onset of EAE. Therefore, we hypothesize that the additional IFN-γ produced by 8.8 CD8+ T cells in the brain may not significantly alter the inflammatory environment established by the donor CD4+ T cells. Furthermore, we would not expect the IFN-γ produced by 8.8 CD8+ T cells to exacerbate atypical CD4-initiated EAE, as we previously showed that IFN-γ exerts an inhibitory influence on brain inflammation in this CD4-initiated EAE model (8).

In contrast to the frequencies of 8.8 CD8+ T cells producing cytokines in the brain, the frequency of CD8+ T cells expressing both FasL and granzyme B in the brain was similar between 8.8 and WT CD8+ T cells. This suggests that these effector molecules are expressed as a result of bystander activation of CD8+ T cells entering the inflamed tissue. Interestingly, despite the antigen-nonspecific manner in which FasL was expressed on 8.8 CD8+ T cells, expression of FasL by 8.8 CD8+ T cells was required to exacerbate atypical EAE. Several observations support the notion that FasL/Fas signaling triggered by cell contact between 8.8 CD8+ T cells and MBP/Kk+ APCs is responsible for the increase in brain inflammation. First, enhanced ROS production occurred only in monocytes and MdCs, which are the cell types that present MBP/Kk, and was not seen in neutrophils or microglia. Second, the increase in proinflammatory ROS expression by monocytes and MdCs mediated by FasL+ 8.8 CD8+ T cells occurred only in the brain and not the spinal cord, like the antigen-specific IFN-γ responses by 8.8 CD8+ T cells. Finally, because similar frequencies were observed for FasL+ WT and 8.8 CD8+ T cells in the brain, it is unlikely that soluble FasL mediated the increased ROS production unless soluble FasL is preferentially secreted by 8.8 versus WT CD8+ T cells.

The increased ROS production by monocytes and MdCs mediated by FasL+ 8.8 CD8+ T cells is consistent with previous reports that macrophages and DCs are relatively resistant to FasL-induced apoptosis. Instead, Fas ligation triggers the production of cytokines, chemokines, and nitric oxide by these cells (41–44). It is possible that Fas ligation on monocytes simultaneously triggers both production of inflammatory mediators and apoptosis, as observed in human monocytes (41). The number of monocytes in the brain increases in mice with CD4-initiated EAE that received 8.8 versus WT CD8+ T cells; however, this could reflect increased recruit-

ment rather than survival of monocytes in the brain. Regardless of whether MBP/K^{k+} monocytes undergo apoptosis as a result of interaction with 8.8 CD8$^+$ T cells, recruitment of 8.8 CD8$^+$ T cells to the brain increases their ROS production. While not addressed in our study, it is also possible that FasL$^+$ 8.8 CD8$^+$ T cells recognize MBP/K^k on Fas-expressing oligodendrocytes and trigger apoptosis in these cells, as we have previously shown that a small percentage of oligodendrocytes also present MBP/K^k (35).

A striking difference exhibited by 8.8 versus WT CD8$^+$ T cells in the CNS is that the frequencies of IFN-γ–, TNF-α–, and FasL-expressing 8.8 CD8$^+$ T cells were significantly higher in the brain compared with the spinal cord (with a similar trend observed for granzyme B), while the frequencies of WT CD8$^+$ T cells expressing these same effector molecules did not differ between the brain and spinal cord. We found that the preferential accumulation of 8.8 CD8$^+$ T cells in the brain was independent of differences in 8.8 CD8$^+$ T cell proliferation or recruitment from the periphery between the brain and spinal cord. It is possible that increased cell death may contribute to the lack of accumulation of 8.8 CD8$^+$ T cells in the spinal cord, if there are intrinsic differences in the manner in which cell death affects accumulation of 8.8 CD8$^+$ T cells versus donor CD4$^+$ T cells in this CNS region. Alternatively, 8.8 CD8$^+$ T cells activated within the spinal cord may migrate to the brain. Future imaging studies that monitor migration of 8.8 CD8$^+$ T cells within different regions of the CNS may address this possibility.

The finding that FasL expression, rather than IFN-γ production, is required to exacerbate atypical CD4-initiated EAE was unexpected and highlights key differences between the pathogenic activities of CD8$^+$ T cells in this scenario versus CNS autoimmunity initiated by CD8$^+$ T cells. We previously showed that adoptive transfer of CD8$^+$ T cell clones specific for the same MBP/K^k epitope as the 8.8 CD8$^+$ T cells induced CNS autoimmunity, and that neutralizing IFN-γ activity within the CNS ameliorated disease severity (28). Importantly, Fas-FasL interactions were not required for the CD8$^+$ T cell clones to initiate disease, as CNS autoimmunity induced in Fas-deficient mice was indistinguishable from the disease induced in WT mice. Here, we found that lytic mechanisms were not essential for 8.8 CD8$^+$ T cells to exacerbate atypical EAE initiated by CD4$^+$ T cells, as perforin expression was not required and recruitment of the 8.8 CD8$^+$ T cells resulted in an increase, rather than a decrease, in the absolute number of MdCs and monocytes in the brain. Instead, a FasL-mediated increase in production of ROS by MdCs and monocytes was sufficient to exacerbate inflammation in the CNS, and this effect was greater in the brain compared with the spinal cord because of increased presentation of the MBP/K^k ligand in the brain. These findings suggest that myelin-specific CD8$^+$ T cells employ distinct effector mechanisms depending on whether they infiltrate a noninflamed environment and initiate disease or are recruited to the CNS after CD4$^+$ T cells have already initiated inflammatory responses.

The proinflammatory activity that we show here for MBP-specific 8.8 CD8$^+$ T cells is also distinct from the recently described activity of CD8$^+$ T cells that undergo oligoclonal expansion in EAE (45). These investigators found that clonally expanded CD8$^+$ T cells observed in EAE correspond to regulatory CD8$^+$ T cells that suppress the activity of the pathogenic CD4$^+$ T cells via cytotoxicity. These CD8$^+$ T cells were not myelin-specific, as they responded

to activated CD4$^+$ T cells, similarly to Qa-1–restricted regulatory CD8$^+$ T cells that recognize MBP-specific CD4$^+$ T cells (46). In contrast, our studies focused on CD8$^+$ T cells that engage in determinant spreading via recognition of MHC class I–restricted myelin epitopes within the CNS. Thus, we would expect the frequency of these myelin-specific CD8$^+$ T cells to be much smaller than that of the regulatory CD8$^+$ T cells that expand in response to the CD4$^+$ T cell population driving disease induction. Despite their low frequency, our data show that these MBP-specific CD8$^+$ T cells exert pathogenic effects in EAE.

In summary, we show here that 8.8 CD8$^+$ T cells play a proinflammatory role in CD4-initiated EAE by preferentially promoting brain inflammation via FasL-mediated increases in ROS production by MdCs and monocytes. Thus, lack of CD8$^+$ T cell involvement in most EAE models may explain some of the discrepancy seen in the lesion distribution between the brain and spinal cord observed in EAE versus MS. Our results suggest that the extent of recruitment of myelin-specific CD8$^+$ T cells to the CNS in individual patients may play a role in determining the prevalence of lesions in the brain.

Methods

Mice. C3HeB/FeJ, CD45.1 (B6.SJL-*Ptprc^a Pepc^b*/BoyJ), *Fasl^{gld}* (C3H/HeJ-*Fasl^{gld}*/J), PFP$^{-/-}$ (C57BL/6-*Prf1tm1^{Sdz}*/J), and Thy1.1 (B6.PL-*Thy1a*/CyJ) mice were originally purchased from The Jackson Laboratory. *Ifng$^{-/-}$* mice were a gift from Christopher B. Wilson at the University of Washington. TCR-transgenic 8.8 mice were previously described (34). CD45.1, Thy1.1, *Ifng$^{-/-}$*, and PFP$^{-/-}$ mice were used after 8 or more backcrosses to the C3HeB/FeJ background. *Tnf$^{-/-}$* mice were generated by the Gene Targeting Facility of the Cancer Research Laboratory at UC Berkeley (Berkeley, California, USA). Two single-guide RNAs (guide 1: AGAAAGCATGATCCGCGACGTGG; guide 2: TCGG-GGTGATCGGTCCCCAAAGG) were injected with Cas9 mRNA into fertilized C3HeB/FeJ zygotes. Mutant mice were identified containing a 165-bp deletion spanning the cytoplasmic and intracellular domains, and a lack of both intracellular and extracellular TNF-α production following T cell stimulation was confirmed by flow cytometry. These mice were bred to 8.8 mice before intercrossing to generate homozygous knockout mice. All mice were bred and maintained in a specific pathogen–free facility at the South Lake Union Campus of the University of Washington.

Protein and peptides. Recombinant rat myelin oligodendrocyte glycoprotein (rMOG; residues 1–125) was produced in *E. coli* as previously described (47). MOG$_{97-114}$ peptide (TCFFRDHSYQEEAAVELK) was purchased from GenScript.

CD8$^+$ T cell enrichment. Single-cell suspensions were prepared from splenocytes from naive C3HeB/FeJ (WT) or 8.8 mice as previously described (12). Cells were labeled with biotinylated antibodies (all from BioLegend) specific for CD4 (RM4-5), B220 (RA3-6B2), CD11b (M1/70), CD11c (N418), and TER-119 (TER-119) and then incubated with magnetic streptavidin particles (557812, BD Biosciences) according to the manufacturer's instructions.

CD4-initiated EAE. EAE was induced in both male and female mice 6–12 weeks of age by adoptive transfer of CD4$^+$ T cells isolated from mice immunized with rMOG and skewed toward a Th17 phenotype in vitro as previously described (9), with slight modifications: spleen and draining lymph nodes were harvested from immunized mice 8

days after immunization. To increase the ability to observe exacerbating effects of 8.8 CD8^{+} T cells on disease, we transferred fewer (2.5×10^5) CD4^{+} blasts (CD4^{+}FSC^{hi}/SSC^{hi}) than in our previous studies (9) in order to establish a less severe disease course in control mice. CD4^{+} T cell blasts were transferred into WT and 8.8 mice that were sublethally irradiated (250 rad) on day –1. To induce CD4-initiated/CD8$_{8.8}$ and CD4-initiated/CD8$_{WT}$ EAE, mice were sublethally irradiated on day –2, and 2×10^6 enriched WT or 8.8 CD8^{+} T cells were transferred i.p. on day –1. CD4^{+} T cell blasts were then transferred i.p. on day 0. Mice were age- and sex-matched between groups and scored for EAE symptoms daily in a blinded manner. Mice were euthanized at a clinical score of ≥5.

Clinical scoring scale. Classic EAE clinical signs were scored as: grade 1, paralyzed tail; grade 2, hind-limb weakness; grade 3, one paralyzed hind limb; grade 4, two paralyzed hind limbs; grade 5, forelimb weakness; grade 6, moribund. Atypical EAE clinical signs were scored as: grade 1, ataxia; grade 2, head tilt; grade 3, mild body lean; grade 4, moderate body lean; grade 5, severe body lean; grade 6, rolling.

Flow cytometry. Single-cell suspensions from the spleen, brain, and spinal cord of perfused mice were prepared as previously described (9). To discriminate live and dead cells, cells were incubated with an amine-reactive dye (Succinimidyl Ester Pacific Orange, Molecular Probes, Invitrogen) for 20 minutes at 4°C. After washing, cells were incubated with Fc block (2.4G2, eBioscience) in 5% mouse serum (MP Biomedicals) for 15 minutes at 4°C, washed, and stained with antibodies for 30 minutes at 4°C. CD4^{+} T cell cytokine production was analyzed after incubation of cells with GolgiPlug (BD Biosciences) and MOG$_{97-114}$ peptide (1 μM) for 4 hours at 37°C. Alternatively, CD8^{+} T cell cytokine production in intact 8.8 mice was analyzed directly ex vivo by incubation of freshly isolated cells with GolgiPlug alone for 4 hours at 37°C. Intracellular cytokine staining was performed using the Cytofix/Cytoperm Kit (BD Biosciences) according to the manufacturer's instructions. Data were acquired with FACSCanto (BD Biosciences) or Aurora (Cytek Biosciences) cytometers and analyzed using FlowJo software (Tree Star).

Antibodies. Antibodies specific for CD4 (RM4-5 and GK1.5), CD45 (30-F11), I-A^k (11-5.2), IFN-γ (XMG1.2), IL-17 (TC11-18H10), Ly6C (AL-21), Ly6G (1A8), Thy1.1 (OX-7), CD62L (MEL-14), and the isotype controls for IFN-γ (rat IgG1, κ) and IL-17 (rat IgG1, κ) were from BD Biosciences. Antibodies specific for CD8 (53-6.7), CD45.1 (A20), CD45.2 (104), TCR-β (H57-597), Thy1.2 (30-H12), TNF-α (MP6-XT22), and the isotype control for TNF-α (rat IgG1, κ) were from BioLegend. Antibodies specific for CD8 (53-6.7), CD11b (M1/70), CD44 (IM7), GM-CSF (MP1-22E9), granzyme B (NGZB), FasL (MFL3), and the isotype for GM-CSF (rat IgG2a, κ) were from eBioscience. Ki67 (SolA15) was from Invitrogen. 12H4 antibody specific for MBP/K^k was generated and validated as previously described (35). For ROS staining, CellROX Deep Red reagent (Life Technologies) was used according to the manufacturer's instructions.

FTY720 injection. CD4-initiated/CD8$_{8.8}$ EAE was induced as described above. On day 6, 3 mg/kg FTY720 (Sigma-Aldrich) or vehicle (5% DMSO) was injected i.p. CNS and spleen mononuclear cells were isolated on day 7 for flow cytometry analysis.

Quantitative reverse transcriptase PCR. Brains and spinal cords of perfused mice with EAE (day 6 after CD4^{+} T cell transfer) or sublethally irradiated healthy control mice were flash-frozen in liquid nitrogen. Tissues were homogenized in QIAzol Lysis Reagent (Qiagen) and total RNA extracted using the RNeasy Lipid Tissue Mini kit (Qiagen). cDNA was synthesized using the SuperScript III first-strand synthesis system (Invi-

trogen). Quantitative reverse transcriptase PCR was performed using SYBR Green Master Mix on a ViiA7 Real-Time PCR system (Applied Biosystems). Data were normalized to *GAPDH* and analyzed using the comparative Ct method. Fold induction of gene expression in EAE mice was calculated relative to expression in sublethally irradiated healthy control mice. Primer sequences are listed in Supplemental Table 1.

Histology. Brains and spinal cords from mice with CD4-initiated EAE (day 7 after CD4^{+} T cell transfer) were fixed in 10% neutral-buffered formalin, sectioned, embedded in paraffin, and stained with H&E. Tissue injury was assessed histologically using a semiquantitative grading system. Approximately 8 evenly distributed cross-sectional areas of each brain were taken from the rostral olfactory region to the caudal portion of the cerebellar cortex. The spinal cord of each mouse was examined using 1.5- to 2-cm long segments of the cervical, thoracic, and lumbar regions. Three H&E-stained histological step sections of each brain area and 1 sagittal section of each spinal cord area were then examined by a board-certified veterinary pathologist who was blinded to group assignments. Lesions were graded for degree of inflammatory cell involvement on an all-inclusive severity scale of 0 (normal) to 4+ (severe). An aggregate histology score for the brain and spinal cord tissue of each mouse was generated by assignment of severity grades for each section that reflected the lesion severity as well as whether the lesions involved the meninges only, meninges and submeningeal regions, or parenchyma surrounding blood vessels (including the perivascular space), and then averaging of these scores. Included in the assessment of inflammation was evaluation for changes consistent with necrosis and apoptosis.

Statistics. EAE incidence and frequencies of parenchymal inflammation were compared using a Fisher's exact test. For all other analyses with 2 groups, comparisons were made using a 2-tailed Mann-Whitney *U* test. For multiple comparisons, Kruskal-Wallis with Dunn's post-test was used. Groups with 2 independent variables were tested using a 2-way ANOVA with Šidák correction for multiple comparisons. Data are presented as 1 symbol per mouse with mean + SEM or mean ± SEM unless otherwise stated in the figure legends. GraphPad Prism 7 was used for all analyses, and *P* values less than 0.05 were considered statistically significant.

Study approval. All procedures were approved by the University of Washington Institutional Animal Care and Use Committee.

Author contributions

CAW designed and performed experiments, analyzed data, and wrote the manuscript. PJR and TRM performed the experiments analyzing MBP/K^k expression. DL carried out the histological analyses. JMG supervised the study and wrote the manuscript.

Acknowledgments

Address correspondence to: Joan M. Goverman, Department of Immunology, University of Washington, Box 358059, 750 Republican Street, Seattle, Washington 98109, USA. Phone: 206.685.7604; Email: goverman@uw.edu.

1. Filippi M, et al. Multiple sclerosis. *Nat Rev Dis Primers*. 2018;4(1):43.

2. Dendrou CA, Fugger L, Friese MA. Immunopathology of multiple sclerosis. *Nat Rev Immunol*. 2015;15(9):545–558.

3. International Multiple Sclerosis Genetics Consortium, et al. Risk alleles for multiple sclerosis identified by a genomewide study. *N Engl J Med*. 2007;357(9):851–862.

4. Goverman J. Autoimmune T cell responses in the central nervous system. *Nat Rev Immunol*. 2009;9(6):393–407.

5. Simmons SB, Pierson ER, Lee SY, Goverman JM. Modeling the heterogeneity of multiple sclerosis in animals. *Trends Immunol*. 2013;34(8):410–422.

6. Segal BM. The diversity of encephalitogenic CD4+ T cells in multiple sclerosis and its animal models. *J Clin Med*. 2019;8(1):E120.

7. Stromnes IM, Cerretti LM, Liggitt D, Harris RA, Goverman JM. Differential regulation of central nervous system autoimmunity by T(H)1 and T(H)17 cells. *Nat Med*. 2008;14(3):337–342.

8. Simmons SB, Liggitt D, Goverman JM. Cytokine-regulated neutrophil recruitment is required for brain but not spinal cord inflammation during experimental autoimmune encephalomyelitis. *J Immunol*. 2014;193(2):555–563.

9. Pierson ER, Goverman JM. GM-CSF is not essential for experimental autoimmune encephalomyelitis but promotes brain-targeted disease. *JCI Insight*. 2017;2(7):e92362.

10. Miller NM, Wang J, Tan Y, Dittel BN. Anti-inflammatory mechanisms of IFN-γ studied in experimental autoimmune encephalomyelitis reveal neutrophils as a potential target in multiple sclerosis. *Front Neurosci*. 2015;9:287.

11. Stromnes IM, Goverman JM. Active induction of experimental allergic encephalomyelitis. *Nat Protoc*. 2006;1(4):1810–1819.

12. Stromnes IM, Goverman JM. Passive induction of experimental allergic encephalomyelitis. *Nat Protoc*. 2006;1(4):1952–1960.

13. Booss J, Esiri MM, Tourtellotte WW, Mason DY. Immunohistological analysis of T lymphocyte subsets in the central nervous system in chronic progressive multiple sclerosis. *J Neurol Sci*. 1983;62(1–3):219–232.

14. Hauser SL, Bhan AK, Gilles F, Kemp M, Kerr C, Weiner HL. Immunohistochemical analysis of the cellular infiltrate in multiple sclerosis lesions. *Ann Neurol*. 1986;19(6):578–587.

15. Babbe H, et al. Clonal expansions of CD8(+) T cells dominate the T cell infiltrate in active multiple sclerosis lesions as shown by micromanipulation and single cell polymerase chain reaction. *J Exp Med*. 2000;192(3):393–404.

16. Jacobsen M, et al. Oligoclonal expansion of memory CD8+ T cells in cerebrospinal fluid from multiple sclerosis patients. *Brain*. 2002;125(pt 3):538–550.

17. Skulina C, et al. Multiple sclerosis: brain-infiltrating CD8+ T cells persist as clonal expansions in the cerebrospinal fluid and blood. *Proc Natl Acad Sci U S A*. 2004;101(8):2428–2433.

18. Junker A, et al. Multiple sclerosis: T-cell receptor expression in distinct brain regions. *Brain*. 2007;130(pt 11):2789–2799.

19. Elong Ngono A, et al. Frequency of circulating autoreactive T cells committed to myelin determinants in relapsing-remitting multiple sclerosis patients. *Clin Immunol*. 2012;144(2):117–126.

20. Crawford MP, et al. High prevalence of autoreactive, neuroantigen-specific CD8+ T cells in multiple sclerosis revealed by novel flow cytometric assay. *Blood*. 2004;103(11):4222–4231.

21. Mars LT, Saikali P, Liblau RS, Arbour N. Contribution of CD8 T lymphocytes to the immuno-pathogenesis of multiple sclerosis and its animal models. *Biochim Biophys Acta*. 2011;1812(2):151–161.

22. Friese MA, et al. Opposing effects of HLA class I molecules in tuning autoreactive CD8+ T cells in multiple sclerosis. *Nat Med*. 2008;14(11):1227–1235.

23. Baughman EJ, et al. Neuroantigen-specific CD8+ regulatory T-cell function is deficient during acute exacerbation of multiple sclerosis. *J Autoimmun*. 2011;36(2):115–124.

24. Cunnusamy K, et al. Disease exacerbation of multiple sclerosis is characterized by loss of terminally differentiated autoregulatory CD8+ T cells. *Clin Immunol*. 2014;152(1–2):115–126.

25. Neumann H, Medana IM, Bauer J, Lassmann H. Cytotoxic T lymphocytes in autoimmune and degenerative CNS diseases. *Trends Neurosci*. 2002;25(6):313–319.

26. Bitsch A, Schuchardt J, Bunkowski S, Kuhlmann T, Brück W. Acute axonal injury in multiple sclerosis. Correlation with demyelination and inflammation. *Brain*. 2000;123(pt 6):1174–1183.

27. Mars LT, et al. CD8 T cell responses to myelin oligodendrocyte glycoprotein-derived peptides in humanized HLA-A*0201-transgenic mice. *J Immunol*. 2007;179(8):5090–5098.

28. Huseby ES, Liggitt D, Brabb T, Schnabel B, Ohlén C, Goverman J. A pathogenic role for myelin-specific CD8(+) T cells in a model for multiple sclerosis. *J Exp Med*. 2001;194(5):669–676.

29. Sun D, et al. Myelin antigen-specific CD8+ T cells are encephalitogenic and produce severe disease in C57BL/6 mice. *J Immunol*. 2001;166(12):7579–7587.

30. Ford ML, Evavold BD. Specificity, magnitude, and kinetics of MOG-specific CD8+ T cell responses during experimental autoimmune encephalomyelitis. *Eur J Immunol*. 2005;35(1):76–85.

31. Ji Q, Perchellet A, Goverman JM. Viral infection triggers central nervous system autoimmunity via activation of CD8+ T cells expressing dual TCRs. *Nat Immunol*. 2010;11(7):628–634.

32. Anderson AC, et al. A transgenic model of central nervous system autoimmunity mediated by CD4+ and CD8+ T and B cells. *J Immunol*. 2012;188(5):2084–2092.

33. Sasaki K, et al. Relapsing-remitting central nervous system autoimmunity mediated by GFAP-specific CD8 T cells. *J Immunol*. 2014;192(7):3029–3042.

34. Perchellet A, Stromnes I, Pang JM, Goverman J. CD8+ T cells maintain tolerance to myelin basic protein by 'epitope theft'. *Nat Immunol*. 2004;5(6):606–614.

35. Ji Q, Castelli L, Goverman JM. MHC class I-restricted myelin epitopes are cross-presented by Tip-DCs that promote determinant spreading to CD8+ T cells. *Nat Immunol*. 2013;14(3):254–261.

36. Steinert EM, et al. Quantifying memory CD8 T cells reveals regionalization of immunosurveillance. *Cell*. 2015;161(4):737–749.

37. Haider L, et al. Oxidative damage in multiple sclerosis lesions. *Brain*. 2011;134(pt 7):1914–1924.

38. Nikić I, et al. A reversible form of axon damage in experimental autoimmune encephalomyelitis and multiple sclerosis. *Nat Med*. 2011;17(4):495–499.

39. van Horssen J, Witte ME, Schreibelt G, de Vries HE. Radical changes in multiple sclerosis pathogenesis. *Biochim Biophys Acta*. 2011;1812(2):141–150.

40. Fischer MT, et al. NADPH oxidase expression in active multiple sclerosis lesions in relation to oxidative tissue damage and mitochondrial injury. *Brain*. 2012;135(pt 3):886–899.

41. Park DR, et al. Fas (CD95) induces proinflammatory cytokine responses by human monocytes and monocyte-derived macrophages. *J Immunol*. 2003;170(12):6209–6216.

42. Ma Y, et al. Fas ligation on macrophages enhances IL-1R1-Toll-like receptor 4 signaling and promotes chronic inflammation. *Nat Immunol*. 2004;5(4):380–387.

43. Chakour R, et al. A new function of the Fas-FasL pathway in macrophage activation. *J Leukoc Biol*. 2009;86(1):81–90.

44. Yi F, Frazzette N, Cruz AC, Klebanoff CA, Siegel RM. Beyond cell death: new functions for TNF family cytokines in autoimmunity and tumor immunotherapy. *Trends Mol Med*. 2018;24(7):642–653.

45. Saligrama N, et al. Opposing T cell responses in experimental autoimmune encephalomyelitis. *Nature*. 2019;572(7770):481–487.

46. Sinha S, Boyden AW, Itani FR, Crawford MP, Karandikar NJ. CD8(+) T-cells as immune regulators of multiple sclerosis. *Front Immunol*. 2015;6:619.

47. Abdul-Majid KB, et al. Screening of several H-2 congenic mouse strains identified H-2(q) mice as highly susceptible to MOG-induced EAE with minimal adjuvant requirement. *J Neuroimmunol*. 2000;111(1–2):23–33.